Experimental Investigations of Discharge Plasma of a Longitudinal Discharge Excimer Laser

縦形放電励起エキシマレーザ中のプラズマの実験的研究

古橋秀夫†、　内田悦行†、　山田諄‡
Hideo FURUHASHI, Yoshiyuki UCHIDA, Jun YAMADA

ABSTRACT *Laser output characteristics of a longitudinal discharge XeCl excimer laser with automatic UV preionization were investigated. The dependences of the laser output peak powers on the buffer gas pressure, the Xe gas pressure and the HCl gas pressure in He/Xe/HCl and Ne/Xe/HCl were measured. The optimum gas mixtures were obtained. Time-dependent particle number densities of the excited components (Xe^{+*}, He*) in the laser were measured by the laser absorption probing with a cw dye laser on the buffer gas pressure, the Xe partial gas pressure and the HCl partial gas pressure. The peak densities of the Xe^{+*} ($6s\,^4P_{3/2}$) ions and the He* ($2p\,^3P$) atoms were about 8×10^{10} cm^{-3} and 7×10^{11} cm^{-3}, respectively The densities were compared with those in transversal discharge XeCl excimer lasers. The formation dynamics of the XeCl excimer molecules, excited atoms and excited ions were discussed. The dependences of the particle number densities of the Xe^{+*} ions on the buffer gas pressure, the Xe gas pressure and the HCl gas pressure were investigated.*

1. INTRODUCTION

Rare gas halide excimer lasers excited by discharge draw attention as a practical high-power UV laser. Transversal discharge excitations have been used for these lasers. On the other hand, in the eighties, some investigations on longitudinal discharge excimer lasers were reported.[1-5] Longitudinal discharge lasers are simple and compact in construction comparing with transversal discharge lasers, and can be useful as compact UV coherent sources.

Although many kinds of preionization techniques are normally used for transversal discharge excimer lasers to obtain uniform and high current discharge, strong preionization such as spark UV preionization has never used for longitudinal discharge rare-gas halide excimer lasers. Therefore, We have proposed a new design of the longitudinal discharge excitation system; longitudinal discharge laser with automatic spark UV preionization. [6]

In the last few years, several investigations of plasma in transversal discharge XeCl excimer lasers[7-12] and electron beam pumped XeCl excimer lasers[13,14] by spectroscopic diagnostic methods have been reported. However, for longitudinal discharge excimer lasers, no investigation of plasma was reported. To clarify the population formation of the excimer in longitudinal discharge excimer lasers and to interpret the difference in the laser output power from transversal discharge excimer lasers, measurements of the plasma discharge parameters are necessary.

In this paper, we report on the laser output

† 愛知工業大学　情報通信工学科　（豊田市）
‡ 愛知工業大学　電子工学科　（豊田市）

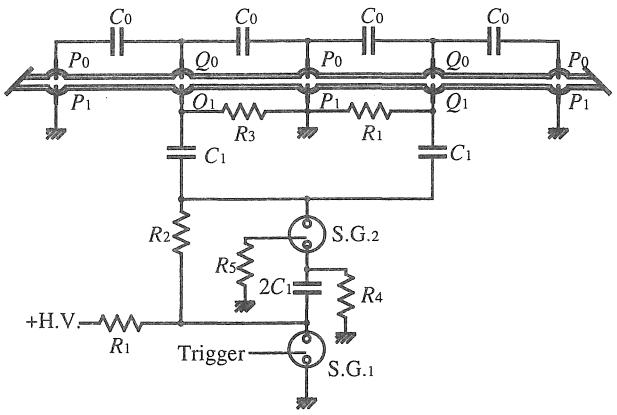

Fig. 1 Schematic diagram of the longitudinal discharge excimer laser. (S.G. : spark gap switch)

characteristics of a longitudinal discharge XeCl excimer laser with automatic spark UV preionization, and the measurements of the time-dependent particle number densities of excited components (Xe^{+}**, He*) in the laser by the laser absorption probing with a cw dye laser. The measured densities are compared with those in transversal discharge XeCl excimer lasers reported before and the difference in laser output power is discussed. The formation dynamics of the XeCl excimer molecules, the excited atoms and the excited ions in the longitudinal discharge XeCl excimer laser are discussed.

2. EXPERIMENTAL

A schematic diagram of the longitudinal discharge XeCl excimer laser with UV spark preionization is shown in Fig. 1. The laser tube employs a four-segment, longitudinal discharge tube. One segment has a length of 65 mm, and thus total length is 260 mm. The inner diameter is 4 mm. Five pairs of electrodes, each of which consists of two stainless pins (P_0-P_1 or Q_0-Q_1) separated by small gap of 4 mm for preionization, are inserted. Since the capacitance of each of the capacitors C_1 is 3.4 nF, the storage capacitance per segment is 850 pF. The capacitance of each of the capacitors C_0 is 560 pF. A two-stage Marx bank generator is used for providing high voltage pulses. The driving voltage is 40 kV.

The optical resonator is composed of two external dielectric mirrors separated by 600 mm, one of which is a total reflector and the other is a 95 % reflecting partial reflector with a 5 m radius of curvature.

When the spark gap switches are closed, a rapidly rising high voltage appears between the electrode pins (P_0-P_1, Q_0-Q_1) through the capacitors C_0. Then these small gaps reach their breakdown voltage and are bridged by sparks. The UV radiation generated by these sparks preionizes the gas in the capillary. At the same time, the capacitors C_0 are charged up by the current from the capacitors C_1. When the preionization proceeds and the capacitors C_0 are charged up to breakdown voltage between the electrode pins P_0 and Q_0, then the main longitudinal discharge occurs along the tube axis, and the capacitors C_0 discharge.

The particle number densities of the excited components were measured by a laser absorption probing spectroscopy. The measurements of the absorption coefficient for lines with known spontaneous transition probabilities A_{ki} allow one to determine the particle number densities of the corresponding excited atoms and ions. The absolute particle number densities of absorbing atoms and ions are given by [15]

$$N = \frac{8\pi g_i}{\lambda^2 A_{ki} g_k} \int k_\nu d\nu \qquad (1)$$

where g_i and g_k are the statistical weight of the states i and k; λ is the wavelength of the investigated transition; A_{ki} is the probabilities of a spontaneous transition; k_ν is the absorption coefficient. In equation (1) it is assumed that the upper level population is small.

Laser light of a cw ring dye laser was used as the light source A cw argon ion laser (Coherent Innova 90-5) was used to pump the dye (Rhodamine 6*G*) optically. A ring dye laser (Coherent Model 7500) provided single frequency operation between 570 nm and 610 nm at a linewidth of 2 GHz (with a three-plate birefringent filter). The laser beam was moved back and forth through the center of the discharge tube. The diameter of the incoming beam waist was about 3 mm. Transmitted laser intensities were measured by a photo-multiplier (Hamamatsu Photonics R448) through a monochromator. The data of 64 measurements at one wavelength were averaged by using a digitizing oscilloscope before subsequent transferal to a microcomputer, and permanent storage on floppy disks. The measurements of the voltage pulses were made with a $CuSO_4$ voltage divider. The voltage between the two electrodes P_1 and Q_1 was used as triggering signals of the oscilloscope. The discharge current pulses were observed using a one-turn Rogowski coil.

3. OPTIMIZATION OF THE GAS MIXTURES

In the case of a XeCl excimer laser excited by discharge, generally a mixture of Xe, HCl and a buffer gas is used. The concentration of these gases has large influences on the laser performance. He, Ne, or Ar is generally used as a buffer gas. Therefore, the gas mixtures are optimized for He/Xe/HCl gas mixtures. Laser oscillation was not obtained for Ar/Xe/HCl gas mixtures.

Figures 2 show the dependence of the laser peak power on the several Xe and HCl partial pressures. In Fig. 2 (a) and (a'), HCl partial pressure is kept constant at 2.4 torr, and Xe partial pressure is changed. In Fig. 2 (b) and (b'), Xe partial pressures are kept constant at 12 torr and 6.0 torr, respectively, and HCl partial pressure is changed. The total gas pressure is varied from 1.0 to 1.5 atm. The optimum partial pressures of Xe and HCl are obtained to be 12 torr and 2.4 torr for Ne/Xe/HCl gas mixture, respectively. On the other hand, the optimum partial pressures of Xe and HCl are obtained to be 6 torr and 2.4 torr for He/Xe/HCl gas mixture, respectively.

There are optimum partial pressures of Xe and HCl. This is because, when the partial pressure of Xe is increased, the formation rate of XeCl* by the following reactions increases.[16]

$$Xe^+ + Cl^- + M \rightarrow XeCl^* + M \qquad (2)$$
$$MXe + Cl^- \rightarrow XeCl^* + M + e \qquad (3)$$
$$Xe^* + HCl(v) \rightarrow XeCl^* + H \qquad (4)$$
$$Xe_2 + Cl^- \rightarrow XeCl^* + Xe + e \qquad (5)$$

M: buffer gas

Furthermore, the electron density increase by the following reactions.[16]

$$Xe^* + e \rightarrow Xe^+ + 2e \qquad (6)$$
$$Xe + e \rightarrow Xe^+ + 2e \qquad (7)$$

However, the discharge impedance decreases at higher Xe partial pressures, and the increase in low energy electrons causes an increase in quenching of XeCl* by the following reaction, which is a dominant loss process of XeCl*.[17]

$$XeCl^* + e \rightarrow Xe + Cl + e \qquad (8)$$

When partial pressure of HCl is increased, the formation rate of XeCl* by the reactions (2)-(5) also increases. However, the electron density decreases by the following dissociative attachment, which is a dominant loss process of electrons.[16]

$$HCl(v) + e \rightarrow H + Cl^- \qquad (9)$$

Furthermore, the photo-absorption of 308 nm laser radiation by following reaction increases.[16]

$$Cl^- + h\nu \rightarrow Cl + e \qquad (10)$$

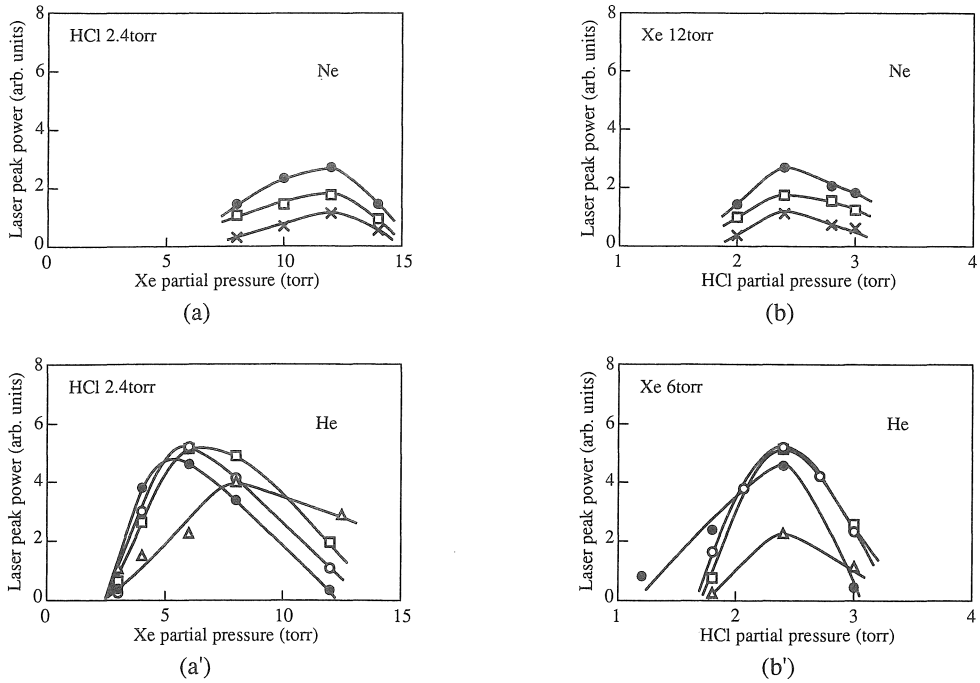

Fig. 2. Dependence of the laser peak powers on the Xe and HCl partial pressures for Ne/Xe/HCl and He/Xe/HCl mixtures. Driving voltage 40 kV. Total gas pressure 1.0 atm (×), 1.2 atm (Δ), 1.3 atm (□), 1.4 atm (○), 1.5 atm (●). Ne: (a) HCl partial pressure 2.4 torr. (b) Xe partial pressure 12 torr. He: (a') HCl partial pressure 2.4 torr. (b') Xe partial pressure 6.0 torr.

At high HCl partial pressure, the quenching of XeCl* by the following reactions increase.[16)]

$$XeCl^* + HCl \rightarrow Xe + Cl + HCl \quad (11)$$
$$XeCl^* + HCl(v) \rightarrow Xe + Cl + HCl \quad (12)$$

Thus, there are optimum partial pressures of Xe and HCl.

Figure 3 shows the comparison of the laser performances using He/Xe/HCl and Ne/Xe/HCl gas mixtures. It shows the dependence of the laser peak power on the buffer gas pressure in the optimum gas mixtures. The driving voltage is 40 kV. The laser peak power using He/Xe/HCl gas mixture is higher than that using Ne/Xe/HCl gas mixture. In a transversal discharge XeCl laser, better laser performance is generally obtained by using Ne/Xe/HCl gas mixture owing to the high reaction rate of the three-body ion-ion recombination (reaction 2). The result obtained in this experiment is probably due to low energy deposition for Ne/Xe/HCl gas mixture. In the case of a longitudinal discharge excimer laser, the electric field is relatively low owing to the long electrode distance. However, high energy deposition is necessary for excimer laser performance owing to the small stimulated emission cross section.[8)] On the other hand, the discharge impedance of Ne/Xe/HCl gas mixture is lower than that of He/Xe/HCl gas mixture.[17,18)] Therefore, the discharge impedance of Ne/Xe/HCl gas mixture below 1.5 atm is lower that the impedance of the external excitation circuit, and the impedances do not match with each other. As a result, the energy deposition for Ne/Xe/HCl gas mixture is lower than that for He/Xe/HCl gas mixture, and the gas mixture is not efficiently excited.

There is an optimum total gas pressure below 1.5 atm for He/Xe/HCl gas mixture, and there will be also an optimum gas pressure over 1.5 atm for Ne/Xe/HCl gas mixture. This is because, when the He (Ne) gas pressure is increased, the XeCl* forma-

tion increases by the three-body ion0ion recombination (reaction 2), but further increase in He (Ne) gas pressure causes a decrease in the electron density and reduction in the electron energy. As a result, the laser peak power decreases at high He (Ne) gas pressure. The difference of the optimum gas pressures for He/Xe/HCl and Ne/Xe/HCl gas mixtures is explained by the difference of the discharge impedance. The discharge impedance of He/Xe/HCl gas mixture matches with the external excitation circuit at low pressures owing to the higher discharge impedance than that of Ne/Xe/HCl gas mixture. However, for Ne/Xe/HCl, the discharge impedance matches with the external excitation circuit at the high pressures owing to the lower discharge impedance. Since it is better to operate the laser at low gas pressure for the compactness of the laser system, it is better to operate the laser at low gas pressure. Therefore, He/Xe/HCl gas mixture is favorable for this purpose.

Maximum laser pulse energy of about 200 μJ was obtained at the driving voltage of 40 kV and using the gas mixtures He : Xe : HCl = 1.4 atm : 6 torr : 2.4 torr. The laser pulse width was about 15 ns (FWHM). Although the output energy is smaller than that of the longitudinal discharge XeCl excimer laser reported by Zhou *et al.* (317μJ output energy, 35 ns pulse width and 30 cm discharge length)[4] owing to the short discharge length, the output power per unit length is 0.5 kW·cm^{-1} and it is larger than that reported them (0.33 kW·cm^{-1}). Furthermore, the efficiency is better than that reported them.

4. MEASUREMENTS OF PARTICLE NUMBER DENSITIES

The particle number densities of the Xe^{+*} ions (6s $^4P_{3/2}$) were measured by using the absorption line 6s $^4P_{3/2} \rightarrow$ 6p $^4P_{3/2}$ (597.65 nm). In the case of transversal discharge excimer lasers, it is considered that the three-body ion-ion recombination shown below is a main reaction of the XeCl* formation in He/Xe/HCl gas mixture.[9]

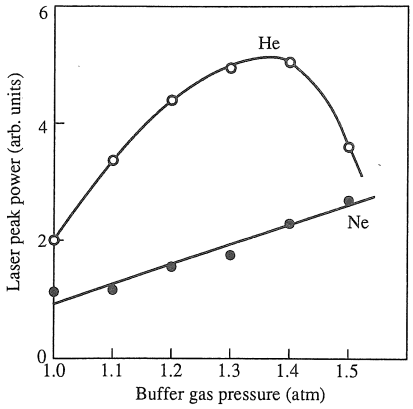

Fig. 3. Dependence of the laser peak power on the buffer gas pressure in the optimum gas mixtures for He and Ne buffer gases. Driving voltage 40 kV. (○) = He buffer, Xe : HCl = 6 torr : 2.4 torr. (●) = Ne buffer, Xe : HCl = 12 torr : 2.4 torr.

$$Xe^+ + Cl^- + He \rightarrow XeCl^* + He \qquad (13)$$

Hence, it is important to measure the densities of the Xe^+ ions to clarify the population formation mechanism. Because the resonant absorption line of the Xe^+ ions in the ground state $5p^5\ ^2P_{3/2}$ is located in the vacuum ultraviolet part of the spectrum, the densities of the Xe^{+*} ions (6s $^4P_{3/2}$) were measured. The densities of the Xe^{+*} ions were also measured before for transversal discharge XeCl excimer lasers.[7-11] Thus, it is possible to discuss the population formation of the longitudinal discharge laser comparing the results with those of transversal discharge excimer lasers. In the case of discharge in low electric field strength such as longitudinal discharge, it seems reasonable to suppose that the Xe^{+*} and Xe^+ ions are formed mainly by stepwise ionization.[16] Thus, the Xe^{+*} ions will show behavior similar to the Xe^+ ions qualitatively.

Figure 4 shows the time behavior of the particle number densities of the Xe^{+*} ions. The gas mixture is He : Xe : HCl = 1.3 atm : 6 torr : 2.4 torr and the driving voltage is 40 kV. The time behavior of the particle number densities of the He* (2p ^3P) atoms, the XeCl* (308.2 nm) spontaneous emission intensities, the discharge voltage, and the discharge current is also represented. Since the voltages be-

tween the electrodes P_1-Q_1 and P_0-Q_0 are different, average value of these voltages is used as the discharge voltage. The densities of the He* (2p ^3P) atoms were measured by using the absorption line 2p $^3P \rightarrow$ 3d ^3D (587.57 nm). Although in the case of the Xe^{+*} density measurements the probing laser beam was moved back and forth in the discharge tube, in the case of the He* density measurements the beam was passed only once because of the large absorption. Since the energy levels of the He* atoms in the 2p $^3P_2$, $^3P_1$, and $^3P_0$ states were close and the absorption line profiles connecting with the upper level overlapped to one another, the densities could not be obtained individually. Therefore, the total densities of He* atoms in the $^3P_2$, $^3P_1$, and $^3P_0$ states were calculated.

The peak densities of the Xe^{+*} (6s $^4P_{3/2}$) ions and the He* (2p ^3P) atoms are about 8×10^{10} cm^{-3} and 7×10^{11} cm^{-3}, respectively. The error in the determination of the absolute densities of excited components is governed primarily by the accuracy of the coefficients A_{ki} and the measured line half-widths. In the case of Xe^{+*} ions and He* atoms, the errors in A_{ki} are 40-50 % [19] and 3 % [20] respectively.

The peaks of the He* densities are caused by the oscillations of the electrical power deposition into discharge. (The first small peak is caused by the spark discharge for the preionization.) The formation of the Xe^{+*} ions starts 15-20 ns after the formation of the He* atoms. This is because the Xe^{+*} ions are not formed by direct impact ionization but by stepwise ionization. Although the Xe^{+*} ions are also formed by the Penning reaction, the ratio is not large because of the low densities of the He* atoms. This Xe^{+*} formation by stepwise ionization coincides with that reported for transversal discharge XeCl excimer lasers.[8,9]

The spontaneous emission of the XeCl* molecules starts soon after the start of the discharge, but rapid increase in the emission starts 20-30 ns after the start of the Xe^{+*} formation and has a maximum later than the maximum of the Xe^{+*} densities. Same behavior was reported also for transversal discharge

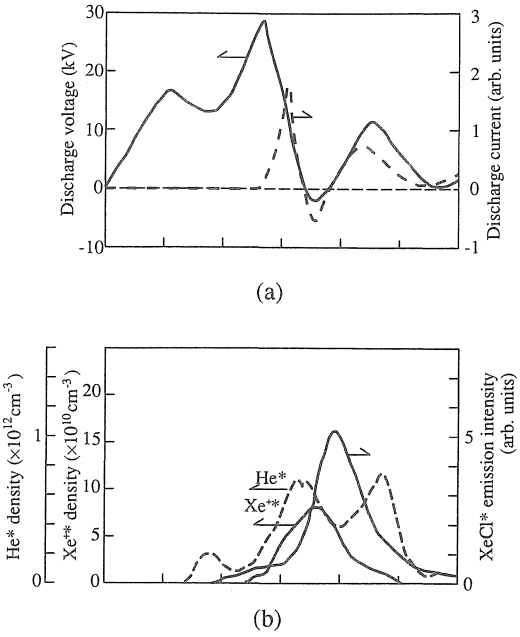

Fig. 4. (a) Time behavior of the discharge voltage, and the discharge current. (b) Time behavior of the particle number densities of the Xe^{+*} 6s $^4P_{3/2}$ ions, that of the He* 2p ^3P atoms, and the spontaneous emission intensity of the XeCl* molecules. He : Xe : HCl = 1.4 atm : 6 torr : 2.4 torr, driving voltage 40 kV. Horizontal axis: 50 ns/div.

XeCl excimer lasers.[7-11] Therefore, the main reaction of the XeCl* formation in the longitudinal discharge laser is three-body ion-ion recombination, that is, the reaction of Xe^+ with Cl^- ions. The formation of the XeCl* molecules at the beginning of the discharge is caused by a harpooning reaction (4) or possibly by the three-body ion-ion recombination (2) with Xe^+ ions in the ground state 5p^5 $^2P_{3/2}$ located at 12 eV below the excited state 6s $^4P_{3/2}$.

Although the specific laser output energies of longitudinal discharge XeCl excimer lasers are a few hundred μJ cm^{-3}, those of typical transversal discharge XeCl excimer lasers are a few mJ cm^{-3}. Next, we will consider this problem. As discussed above, since the reaction of the XeCl* formation in the longitudinal discharge laser is similar to that in transversal discharge XeCl excimer lasers, that is, the main process is three-body ion-ion recombination with Xe^+, Cl^- ions and He atoms, the densities

of these ions and atoms are closely concerned with the laser output power. The densities of transversal discharge excimer lasers in the 6s $^4P_{5/2}$ state were reported to be 5 - 6 cm^{-3}.[7,9] (It is located at 0.25 eV below the 6s $^4P_{3/2}$ state. The densities in the 6s $^4P_{3/2}$ state have not been reported before.) However, the XeCl* formation rate is determined by the product of the densities of the Xe^+, Cl^- ions and the He atoms. Although the optimum gas pressure (He pressure) of the longitudinal discharge laser is around 1 atm, those of transversal discharge lasers are around 4 atm. Therefore, the densities of He atoms in the longitudinal discharge laser is low and, as a result, the XeCl* formation rate is small.

In a longitudinal discharge tube, the role of the walls of the tube is of interest, because the discharge touches the wall directly. Laser beams in the shape of a hollow cylinder have been reported in longitudinal discharge lasers.[4] This is probably caused by concentration of the discharge near the discharge tube owing to the skin effect or the creeping discharge. Low output energies of longitudinal discharge lasers may be due to the concentration of the discharge and low electron densities at the center of the discharge tube. However, in this experiment, the output laser beams had circular cross sections, and the densities of the Xe^{+*} ions are not low. Therefore, the excitation is not hardly affected by the walls of the discharge tube used in its experiment.

It has been considered that the low optimum gas pressure of longitudinal discharge lasers is due to the existence of the optimum E/P value (where E is electric field strength and P is gas pressure) of these types of lasers, when considering only the external parameters. The electron temperature decreases with the decrease in the E/P value. The discharge gaps of longitudinal discharge lasers are longer than those of transversal discharge lasers. Therefore, the electric field strength E is low and the gas pressure must be low to operate at the optimum E/P value. However, discharge voltage changes with time and the relation between the plasma condition and gas pressure is not interpreted in detail.

Figure 5 shows the dependence of the particle number densities of the Xe^{+*} ions (6s $^4P_{3/2}$) on the He gas pressure. The Xe and HCl partial pressures were kept 6 torr and 2.4 torr respectively and He partial gas pressure was varied. With the increase in the He gas pressure, the laser peak output power increases until reaching 1.4 atm and then decreases. On the other hand, the densities of the Xe^{+*} ions (6s $^4P_{3/2}$) increase with the increase in the He gas pressure. Therefore, the decrease in the peak laser output power above the optimum gas pressure is not caused by the decrease in the densities of the Xe^+ ions.

Although the dependence of the Xe^{+*} ions on the buffer gas pressure has not been reported before, Hammer et al. obtained the particle number densities of the Xe* atoms in a transversal discharge XeCl excimer laser using Ne buffer gas by model calculations. They reported that the densities increase with the increase in the buffer gas pressure.[12] (Experimentally, they obtained opposite buffer gas pressure dependence.) This dependence of the densities on the buffer gas pressure is due to the increase in the discharge voltage, the electron densities, and the input power densities with the increase in the buffer gas pressure.

Figure 6 shows the dependence of the particle number densities of the Xe^{+*} (6s $^4P_{3/2}$) ions on the

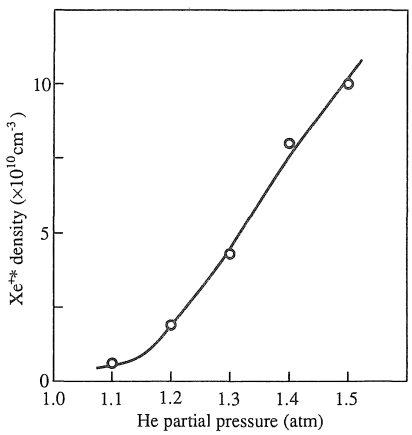

Fig. 5. Dependence of the particle number densities of the Xe^{+*} 6s $^4P_{3/2}$ ions on the He gas pressure. Xe : HCl = 6 torr : 2.4 torr, driving voltage 40 kV.

Xe partial gas pressure. The He and HCl partial gas pressures were kept 1.4 atm and 2.4 torr respectively, and the Xe partial gas pressure was varied. The densities of the Xe^{+*} ions increase with the increase in the Xe partial gas pressure until reaching 6 torr and then are saturated. This is because, at the low Xe partial gas pressure, the densities of the Xe^{+*} ions increase owing to the increase in the collision of the Xe atoms with the electrons with the increase in the Xe partial gas pressure. However, the increase in the Xe partial gas pressure causes an increase in the electron densities (discharge current) and a decrease in the discharge impedance. As a result, the discharge voltage drops and the densities of the Xe^{+*} ions are saturated.

Above 6 torr the concentration of the Xe^{+} ($5p^5\ {}^2P_{3/2}$) ions increases and that of the Xe^{+*} ($6s\ {}^4P_{3/2}$) ions decreases due to the decrease in the electron energy. The peak laser output power increases with the increase in the Xe partial gas pressure until reaching 6 torr and then decreases. The optimum Xe partial gas pressure for obtaining the maximum laser peak power almost agrees with the gas pressure at which the Xe^{+*} ion densities are saturated. Above 6 torr, the increase in the Xe partial gas pressure increases the collisional quenching of the XeCl* excimer molecules with Xe atoms and electrons, and the laser peak power decreases.

Figure 7 shows the dependence of the particle number densities of the Xe^{+*} ($6s\ {}^4P_{3/2}$) ions on the HCl partial gas pressure. The He and Xe partial gas pressures were kept 1.4 atm and 6 torr respectively, and the HCl partial gas pressure was varied. The densities of the Xe^{+*} ions decrease with the increase in the HCl partial gas pressure. This is because, when the HCl partial gas pressure is increased, the decay rate of the Xe^{+} ions by the XeCl* formation increases owing to the increase in the Cl^- ions. Furthermore, electron densities decrease owing to the electron attachment with HCl, and electron energy decreases owing to the inelastic collision cooling by HCl. Figure 8 shows the rate coefficients of Xe excitation and Xe* ionization as a function of the HCl partial gas pressure in Ne/Xe/HCl laser mixture for a transversal discharge laser.[21] As shown in this figure, the rate coefficients decrease with HCl. This fact supports the forgoing argument.

The peak laser output power increases with the increase in the HCl partial gas pressure until reaching 2.4 torr and then decreases. This is because, at low HCl partial gas pressure the formation rate of the Cl^- ions increases with the increase in the HCl partial gas pressure. However, at high HCl partial gas pressure, the densities of the Xe^{+} ions decrease and the Cl^- ions which are not used for the XeCl* excimer formation absorb the XeCl* excimer emission.

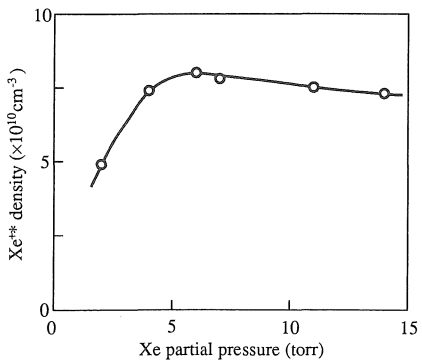

Fig. 6. Dependence of the particle number densities of the Xe^{+*} 6s $^4P_{3/2}$ ions on the Xe gas pressure. He : HCl = 1.4 atm : 2.4 torr, driving voltage 40 kV.

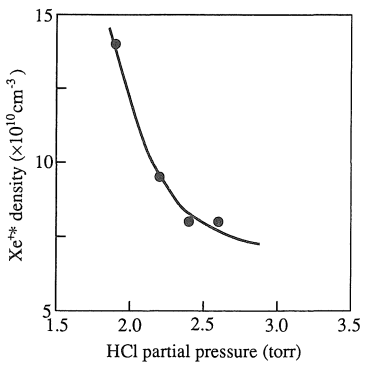

Fig. 7. Dependence of the particle number densities of the Xe^{+*} 6s $^4P_{3/2}$ ions on the HCl gas pressure. He : Xe = 1.4 atm : 6 torr, driving voltage 40 kV.

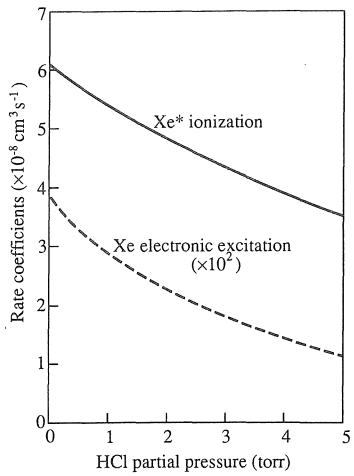

Fig. 8. Dependence of the particle number densities of the Xe* ionization rate coefficients and Xe electronic excitation coefficients on the HCl gas pressure reported by Longo *et al.*[21]

5. CONCLUSION

We have studied on the laser output characteristics of a longitudinal discharge XeCl excimer laser with automatic UV preionization. The dependence of the laser output peak powers on the buffer gas pressure, the Xe gas pressure and HCl gas pressure in He/Xe/HCl and Ne/Xe/HCl were investigated. Laser beam of 200 μJ output energy and 15 ns width (FWHM) was obtained with the gas mixture of He : Xe : HCl = 1.4 atm : 6 torr : 2.4 torr. We have also measured the time-dependent particle number densities of the excited components (Xe^{+*}, He*) in the laser by the laser absorption probing with a cw dye laser operating in the range of 570-610 nm. The time-dependent densities have been compared with those in transversal discharge XeCl excimer lasers reported before. It has been shown that three-body ion-ion recombination is a main reaction of the XeCl* formation, which is also a main reaction in transversal discharge XeCl excimer lasers. Since the particle number densities of the Xe^{+*} ions in the longitudinal discharge laser are of the same order of magnitude as those of transversal discharge lasers, the low specific laser output energy of the longitudinal discharge laser is not due to the low Xe^{+*} ion densities. The dependence of the particle number densities of the Xe^{+*} ions on the buffer gas pressure, the Xe partial gas pressure and the HCl partial gas pressure has been investigated. To discuss the population formation of the excimer in longitudinal discharge excimer lasers in more detail, it is desirable that the particle number densities of the Cl^- ions, Xe* atoms, HCl(v) molecules, and electron densities will be measured.

ACKNOWLEDGMENTS

The research was supported in part by a Grant-in-Aid for Scientific Research from Ministry of Education, Science and Culture, Japan and in part by the Naito Research Grant.

REFERENCES

1) I. M. Isakov and A. G. Leonov, V. E. Ogluzdin: Excitation of a XeF laser with a longitudinal electric discharge, Sov. Tech. Phys. Lett., **3**(9), 397-398, 1977.
2) P. Burkhard, T. Geber and W. Lüthy: XeF excimer laser pumped in a longitudinal low-pressure discharge, Appl. Phys. Lett., **39**(1), 19-20, (1981).
3) D. Cleshinsky, D. Dammasch, H. J. Eichler and J. Hamisch: XeF laser with longitudinal discharge excitation, Opt. Commun., **39**(1,2), 79-82, (1981).
4) Z. Zhou, Y. Zeng and M. Qiu: XeCl excimer laser excited by longitudinal discharge, Appl. Phys. Lett., **43**(4), 347-349, 1983.
5) H. J. Eichler, J. Hamisch, B. Nagel and W. Schmid: KrF laser with longitudinal discharge excitation, Appl. Phys. Lett., **46**(10), 911-913 (1985).
6) H. Furuhashi, M. Hiramatsu and T. Goto: Longitudinal discharge XeCl excimer laser with automatic UV preionization, Appl. Phys. Lett., **50**(14), 883-885, 1987.
7) D. C. Hogan, A. J. Kearsley, C. E. Webb and R. Bruzzese: Time-resolved measurements of emission and absorption in a long pulse duration XeCl* laser, J. Physique, **45**, 1449-1456, 1984.
8) V. É. Peét and A. B. Treshchalov: Investigation of the dynamics of formation of excited atoms, ions, and excimer molecules in the plasma of an electric-discharge XeCl laser, Sov. J. Quantum Electron., **15**(12), 1613-1619, 1985.
9) A. B. Treshchalov, V. É. Peét and V. T. Mihkelsoo: Formation dynamics of excited components in discharge XeCl laser plasma from the data of dye laser absorption

probing, IEEE J. Quantum Electron., **QE-22**(1), 51-57, 1986.

10) A. V. Dem'yanov, V. S. Aggrieve, I. V. Kochetov, A. P. Napartovich, A. A. Pastor, N. P. Penkin, P. Yu. Serdobintsen and N. N. Shubin: Investigation of the dynamics of the populations of electronic states of atoms and ions in a self-sustained discharge in an HCl-Xe-He mixture, Sov. J. Quantum Electron., **16**(6), 817 -820, 1986.

11) A. B. Treshchalov and V. É. Peét: Spatial-time dynamics of the discharge pumping and lasing in a XeCl excimer laser, IEEE J. Quantum Electron., **24**(2), 169-176, 1988.

12) Th. Hammer and W. Bötticher: Spectroscopic investigation of the ionization kinetics in XeCl laser discharges by Xe* density measurements, Appl. Phys. B, **48**, 73-84, 1989.

13) F. Kannari, W. D. Kimura, J. F. Seamans and D. R. Guyer: Xenon excited state density measurements in electron beam pumped XeCl laser mixtures, Appl. Phys. Lett., **51**(24), 1986-1988, 1987.

14) F. Kannari, W. D. Kimura, J. F. Seamans and D. R. Guyer: Xenon excited-densities in electron-beam pumped XeCl and XeF, J. Appl. Phys., **64**(2), 507-515, 1988.

15) A. C. G. Mitchell and M. W. Zemansky: *Resonance Radiation and Excited Atoms*. Cambridge University Press, London, 1934.

16) M. Ohwa and M. Obara: Theoretical analysis of efficiency scaling laws for a self-sustained discharge pumped XeCl laser, J. Appl. Phys., **59**(1), 32-41, 1986.

17) H. Hokazono, K. Midorikawa, M. Obara and T. Fujioka: Theoretical analysis of a self-sustained discharge pumped XeCl laser, J. Appl. Phys., **56**(3), 680-690, 1984.

18) M. Hiramatsu, H. Furuhashi and T. Goto: Determination of electron density in discharge-pumped excimer laser using Stark broadening of H_β line, J. Appl. Phys., **59**(6), 1946-1948, (1986).

19) M. H. Miller, R. A. Roig, R. D. Bengtson: Transition probabilities of Xe I and Xe II, Phys. Rev. A, **8**, 480-486, 1973.

20) W. L. Wiese, M. W. Smith, B. M. Glenon, *Atomic transition probabilities - Hydrogen through Neon*, (NSRDS-NBS 4), National Bureau of Standards, Washington, DC. **1**, 9-15, 1966.

21) S. Longo, C. Gorse and M. Capitelli: Open problems in the XeCl laser physics, IEEE Trans. Plasma Science, **19**, 379-386, 1991.

（受理 平成６年３月２０日）